Article ID: 1007-4627(2017) 01-0029-06

Nuclear Fragmentation and Particle Production Induced by Antiprotons

FENG Zhaoqing

(*Institute of Modern Physics, Chinese Academy of Sciences, Lanzhou 730000, China*)

Abstract: Within the framework of the Lanzhou quantum molecular dynamics (LQMD) transport model, the nuclear fragmentation and particle production induced by low-energy antiprotons have been investigated thoroughly. Production of strange particles in the antiproton induced nuclear reactions is modeled within the LQMD model, in which all possible reaction channels such as elastic scattering, annihilation, charge exchange and inelastic scattering in antibaryon-baryon, baryon-baryon and meson-baryon collisions have been included. A coalescence approach is developed for constructing the primary fragments in phase space. The secondary decay process of the fragments is described by the well-known statistical code. It is found that the strangeness exchange reactions dominate the hyperon production. A bump structure in the domain of intermediate mass for heavy targets appears owing to the contribution of fission fragments. It has advantage to produce heavier hyperfragments and hypernuclides with strangeness $s=-2$ (double-Λ fragments) and $s=1$ ($\overline{\Lambda}$-fragments) in antiproton induced reactions. The production cross sections are evaluated.

Key words: LQMD transport model; particle production; nuclear fragmentation; antiproton induced reaction

CLC number: O571.6 **Document code:** A **DOI:** 10.11804/NuclPhysRev.34.01.029

1 Introduction

The nuclear dynamics induced by antiproton-nucleus collisions is a complex process, which is associated with the mean-field potentials of antinucleons and produced particles in nuclear medium, and also with a number of reaction channels, *i.e.*, the annihilation channels, charge-exchange reaction, elastic and inelastic collisions. The cold quark-gluon plasma (QGP) could be formed from the annihilation of antiprotons on nuclei[1] and the searching is still undergoing in experiments. The large yields of strange particles may be produced in antiproton induced reactions, which have the advantage to produce in comparison to proton-nucleus and heavy-ion collisions. Studies of hypernuclei attract much attention over the past several decades. The interested topics related to hypernuclei are the hyperon-nucleon and hyperon-hyperon interactions, opening a new horizon with strangeness (three-dimensional nuclear chart) in nuclear physics and probing the in-medium properties of hadrons and the inner structure of a nucleus[2, 3]. Since the first observation of Λ-hypernuclides in nuclear multifragmentation reactions induced by cosmic rays in 1950s[4], a remarkable progress has been obtained in producing hypernuclides via different reaction mechanism, such as hadron (pion, kaon, proton) induced reactions, bombarding a fixed target with high-energy photons or electrons, and fragmentation reactions with high energy heavy-ion collisions.

A more localized energy deposition enables the secondary collisions available for producing hyperons. Hyperons produced in antiproton induced reactions can be captured in the potential of nucleon fragments to form hypernuclei. The dynamics of antiproton-nucleus collisions is complicated, which is associated with the mean-field potentials of hadrons in nuclear medium, and also with a number of reaction channels, *i.e.*, the annihilation channels, charge-exchange reaction, elastic and inelastic collisions. The larger yields of strange particles in antiproton induced reactions are favorable to form hypernuclei in compar-

Received date: 18 Sep. 2016

Foundation item: National Natural Science Foundation of China(11675226, 11175218); National Basic Research Program of China(973 Program)(2015CB856903); Youth Innovation Promotion Association of Chinese Academy of Sciences

Biography: FENG Zhaoqing (1979–), male, Dingxi, Gansu, Researcher, working on nuclear physics;
E-mail: fengzhq@impcas.ac.cn.

ison to proton-nucleus and heavy-ion collisions. To understand the nuclear dynamics induced by antiprotons, several approaches have been proposed, such as the intranuclear cascade (INC) model[5], kinetic approach[6], Giessen Boltzmann-Uehling-Uhlenbeck (GiBUU) transport model[7], Statistical Multifragmentation Model (SMM)[8] and the Lanzhou quantum molecular dynamics (LQMD) approach[9]. A number of experimental data were nicely explained within these approaches. Self-consistent description of dynamical evolutions and collisions of antiproton on nucleus is still very necessary, in particular for understanding the fragmentation reactions in collisions of antiprotons on nuclei to form hypernuclei. The production of hypernuclei is associated with the reaction channels of hyperons, and also related to the hyperon-nucleon (HN) and hyperon-hyperon (HH) potentials. The investigation of hypernucleus properties is an essential way for extracting the in-medium information of hyperons.

2 Brief description of the model

In the LQMD model, the dynamics of resonances ($\Delta(1232)$, N*(1440), N*(1535) *etc*), hyperons (Λ, Σ, Ξ) and mesons (π, K, η, $\overline{\mathrm{K}}$, ρ, ω, ϕ *etc*) is described via hadron-hadron collisions, annihilation reactions of antibaryon-baryon collisions, decays of resonances and transportation in mean-field potentials[10, 11]. The temporal evolutions of baryons (nucleons, resonances and hyperons), anti-baryons and mesons in the nuclear collisions are governed by Hamilton's equations of motion. The Hamiltonian of nucleons and nucleonic resonances is derived from the Skyrme energy-density functional and a momentum-dependent potential distinguishing isospin effects has been implemented in the model.

Dynamics of hyperons and mesons is described within the framework of relativistic mean-field models or chiral perturbation theories[12]. The antibaryon energy is computed from the G-parity transformation of baryon potential as

$$\omega_{\overline{\mathrm{B}}}(\boldsymbol{p}_i,\rho_i)=\sqrt{(m_{\overline{\mathrm{B}}}+\Sigma_{\mathrm{S}}^{\overline{\mathrm{B}}})^2+\boldsymbol{p}_i^2}+\Sigma_{\mathrm{V}}^{\overline{\mathrm{B}}} \tag{1}$$

with $\Sigma_{\mathrm{S}}^{\overline{\mathrm{B}}}=\Sigma_{\mathrm{S}}^{\mathrm{B}}$ and $\Sigma_{\mathrm{V}}^{\overline{\mathrm{B}}}=-\Sigma_{\mathrm{V}}^{\mathrm{B}}$. The nuclear scalar $\Sigma_{\mathrm{S}}^{\mathrm{N}}$ and vector $\Sigma_{\mathrm{V}}^{\mathrm{N}}$ self-energies are computed from the well-known relativistic mean-field model with the NL3 parameter ($g_{\sigma\mathrm{N}}^2=80.8$, $g_{\omega\mathrm{N}}^2=155$ and $g_{\rho\mathrm{N}}^2=20$). The optical potential of baryon or antibaryon is derived from the in-medium energy as $V_{\mathrm{opt}}(\boldsymbol{p},\rho)=\omega(\boldsymbol{p},\rho)-\sqrt{\boldsymbol{p}^2+m^2}$. The relativistic self-energies are used for the construction of hyperon and antibaryon potentials only. A very deep antiproton-nucleus potential is obtained with the G-parity approach being $V_{\mathrm{opt}}(\mathbf{p}=0,\rho=\rho_0)=-655$ MeV. From fitting the antiproton-nucleus scattering[7] and the real part of phenomenological antinucleon-nucleon optical potential[13], a factor ξ is introduced in order to moderately evaluate the optical potential as $\Sigma_{\mathrm{S}}^{\overline{\mathrm{N}}}=\xi\Sigma_{\mathrm{S}}^{\mathrm{N}}$ and $\Sigma_{\mathrm{V}}^{\overline{\mathrm{N}}}=-\xi\Sigma_{\mathrm{V}}^{\mathrm{N}}$ with $\xi=0.25$, which leads to the strength of $V_{\overline{N}}=-164$ MeV at the normal nuclear density $\rho_0=0.16$ fm^{-3}. It should be noted that the scaling approach violates the fundamental G-symmetry. The antihyperon potentials exhibit strongly attractive interaction in nuclear medium, *e.g.*, the strengths at saturation density being -436 MeV and -218 MeV for $\overline{\Lambda}$ and $\overline{\Xi}$, respectively. The optical potentials will affect the dynamics of hyperons, consequently the production of hypernuclei.

The scattering in two-particle collisions is performed by using a Monte Carlo procedure, in which the probability to be a channel in a collision is calculated by its contribution of the channel cross section to the total cross section. The primary products in nucleon-nucleon (NN) collisions are the resonances of $\Delta(1232)$, N*(1440), and N*(1535). We have included the reaction channels as follows:

$$\begin{aligned}&\mathrm{NN}\leftrightarrow\mathrm{N}\triangle,\ \mathrm{NN}\leftrightarrow\mathrm{NN}^*,\ \mathrm{NN}\leftrightarrow\triangle\triangle\ ,\\&\Delta\leftrightarrow\mathrm{N}\pi,\mathrm{N}^*\leftrightarrow\mathrm{N}\pi,\mathrm{NN}\leftrightarrow\mathrm{NN}\pi(\text{s-state})\ ,\\&\mathrm{N}^*(1535)\leftrightarrow\mathrm{N}\eta\ .\end{aligned} \tag{2}$$

Here hadron-hadron collisions take place as two-body process and three-body (s-state pion production) reactions. At the considered energies, there are mostly Δ resonances which disintegrate into a π and a nucleon in the evolutions. The momentum-dependent decay widths are used for the resonances of $\Delta(1232)$ and N*(1440)[10]. We have taken a constant width of $\Gamma=150$ MeV for the N*(1535) decay. Elastic scattering of NN, nucleon-resonance (NR $\rightarrow$ NR) and resonance-resonance (RR $\rightarrow$ RR) collisions and inelastic collisions of nucleon-resonance (NR $\rightarrow$ N, NR $\rightarrow$ NR′) and resonance-resonance (RR $\rightarrow$ N, RR $\rightarrow$ RR′, R and R′ being different resonances), have been included in the model.

The strangeness and vector mesons (ρ, ω) are created in inelastic hadron-hadron collisions without intermediate resonances. We included the channels as follows:

$$\begin{aligned}&\mathrm{BB}\rightarrow\mathrm{BYK},\mathrm{BB}\rightarrow\mathrm{BBK}\overline{\mathrm{K}},\mathrm{B}\pi(\eta)\rightarrow\mathrm{YK},\mathrm{YK}\rightarrow\mathrm{B}\pi\ ,\\&\mathrm{B}\pi\rightarrow\mathrm{NK}\overline{\mathrm{K}},\mathrm{Y}\pi\rightarrow\mathrm{B}\overline{\mathrm{K}},\mathrm{B}\overline{\mathrm{K}}\rightarrow\mathrm{Y}\pi,\mathrm{YN}\rightarrow\overline{\mathrm{K}}\mathrm{NN}\ ,\\&\mathrm{NN}\rightarrow\mathrm{NN}\rho,\mathrm{NN}\rightarrow\mathrm{NN}\omega\ .\end{aligned} \tag{3}$$

Here the B stands for (N, $\triangle$, N*) and Y(Λ, Σ), K(K^0, K$^+$) and $\overline{\mathrm{K}}$($\overline{\mathrm{K}}^0$, K$^-$). Furthermore, the elastic

scattering and strangeness-exchange reaction between strangeness and baryons have been considered through the channels of KB → KB, YB → YB and $\overline{\mathrm{K}}\mathrm{B} \to \overline{\mathrm{K}}\mathrm{B}$. The charge-exchange reactions between the KN → KN and YN → YN channels are included by using the same cross sections with the elastic scattering, such as $\mathrm{K}^0\mathrm{p} \to \mathrm{K}^+\mathrm{n}$, $\mathrm{K}^+\mathrm{n} \to \mathrm{K}^0\mathrm{p}$ *etc*[11].

Based on hadron-hadron collisions, to describe the antiproton-nucleus collisions we have further included the annihilation channels, charge-exchange reaction (CEX), elastic (EL) and inelastic scattering as follows[9]:

$$\begin{aligned}&\overline{\mathrm{B}}\mathrm{B} \to \text{annihilation}(\pi,\eta,\rho,\omega,\mathrm{K},\overline{\mathrm{K}},\eta',\mathrm{K}^*,\overline{\mathrm{K}}^*,\phi)\ ,\\&\overline{\mathrm{B}}\mathrm{B} \to \overline{\mathrm{B}}\mathrm{B}(\text{CEX, EL}),\ \overline{\mathrm{N}}\mathrm{N} \leftrightarrow \overline{\mathrm{N}}\Delta(\overline{\Delta}\mathrm{N})\ ,\\&\overline{\mathrm{B}}\mathrm{B} \to \overline{\mathrm{Y}}\mathrm{Y}\ .\end{aligned} \tag{4}$$

Here the B strands for nucleon and Δ(1232), Y(Λ, Σ, Ξ), K(K^0, K^+) and $\overline{\mathrm{K}}$($\overline{\mathrm{K}^0}$, K^-). The overline of B (Y) means its antiparticle. The cross sections of these channels are based on the parametrization or extrapolation from available experimental data[14]. The annihilation dynamics in antibaryon-baryon collisions is described by a statistical model with $SU(3)$ symmetry inclusion of all pseudoscalar and vector mesons[15], which considers various combinations of possible mesons with the final state from two to six particles[16]. Pions are the dominant mesons in the annihilation of antiproton on a nucleus. The averaged number is about 3 ∼ 4 per antiproton. Shown in Fig. 1 is a schematic picture in low-energy antiproton induced nuclear reactions. The fragmentation process can be understood as three stages, antiproton-nucleon annihilation (energy released), pion-nucleon collisions (energy deposited) and fragmentation of highly excited nucleus (nuclear explosion). The total multiplicities of particles in antiproton induced reactions on different target are presented in Table 1. It is interesting to find that the pions, kaons and hyperons increase with the mass of target nucleus. However, the yields of antikaons are reduced with the target becoming heavier. At the considered energy below its threshold energy, *e.g.*, the reaction $\overline{\mathrm{N}}\mathrm{N} \to \overline{\Lambda}\Lambda$ ($\mathrm{p}_{\mathrm{threshold}} = 1.439$ GeV/c), hyperons are mainly contributed from the secondary collisions, *i.e.*, $\pi\mathrm{N} \to \mathrm{KY}$ and $\overline{\mathrm{K}}\mathrm{N} \to \pi\mathrm{Y}$. The heavier target enhances the collision probability, which are available for producing hyperons.

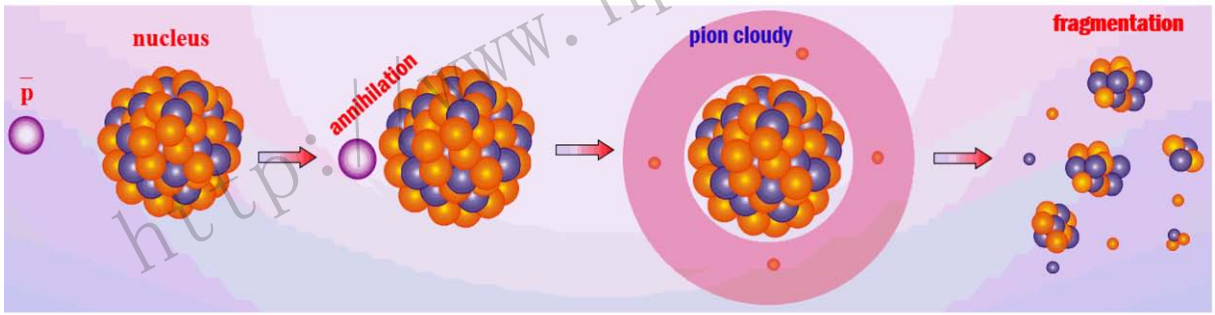

Fig. 1　(color online) Schematic picture in collisions of $\overline{\mathrm{p}}$ on a nucleus.

Table 1　The total multiplicities of particles produced in the antiproton induced reactions on ^{12}C and ^{197}Au at an incident energy of 21 MeV.

Target	π^+	π^0	π^-	K^+	K^0	K^-	$\overline{\mathrm{K}}^0$	$\Lambda+\Sigma^0$	Σ^+	Σ^-
^{12}C	0.6	1.2	1.5	0.027	0.034	0.013	0.008	0.021	0.009	0.010
^{197}Au	0.8	1.4	1.6	0.045	0.051	0.010	0.007	0.051	0.011	0.017

3　Results and discussions

The localized energy is deposited in nuclei via particle-nucleon collisions. Roughly, the energy released by stopped antiprotons on Au is similar to that irradiated by 1 GeV protons[17]. Besides a number of mesons emitted after the annihilation of antiprotons in nuclei, target nuclei are excited with the energy deposition, which leads to evaporate nucleons and clusters from the transient nuclei and even to fragmentation reactions. The nuclear dynamics induced by antiprotons is described by the LQMD model. The primary fragments are constructed in phase space with a coalescence model, in which nucleons at the freeze-out stage (equilibrium state for particle production) are considered to belong to one cluster with the relative momentum smaller than P_0 and with the relative distance smaller than R_0 (here $P_0 = 200$ MeV/c and $R_0 = 3$ fm). The primary fragments are highly excited. The de-excitation of the fragments is assumed to be isolated without rotation (zero angular momentum) and evaluated with the statistical code GEMINI[18]. The exci-

tation energy is evaluated as the difference of binding energies between the excited fragment and its ground state ones. Shown in Fig. 2 is the excitation energy distributions in antiproton induced reactions. The average excitation energies are 42.4 MeV and 264.6 MeV for the target nuclei ^{63}Cu and ^{181}Ta, respectively, which are evaluated from the formula of $< E^* >= \int E^*\sigma(E^*)\mathrm{d}E^* / \int \sigma(E^*)\mathrm{d}E^*$, and $\sigma(E^*)$ being the sum of cross sections of fragments with $Z \geqslant 6$ at the excitation energy of E^*.

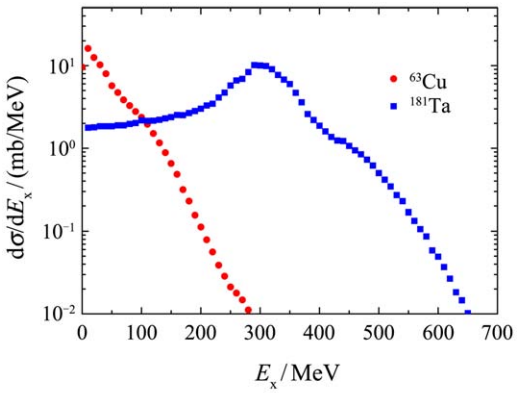

Fig. 2 (color online) Excitation distributions in the annihilation of antiprotons on ^{63}Cu and ^{181}Ta, respectively.

As a test of the model, the fragmentation reactions induced by antiprotons are investigated. Fragment distributions is presented in Fig. 3. The secondary decay of primary fragments leads to the appearance of the bump structure around $A \sim 70$ and $Z \sim 32$, which comes from the fission of target-like fragments. The fragmentation reactions with low-energy antiprotons were investigated at the low-energy antiproton ring (LEAR) at CERN. Comparison of the calculations with the LEAR data is shown in Fig. 4. It is obvious that the mass spectra are nicely reproduced with the combined approach. The fragmentation undergoes the processes of pre-equilibrium particle emissions, fission, evaporation of nucleons and light fragments *etc.*

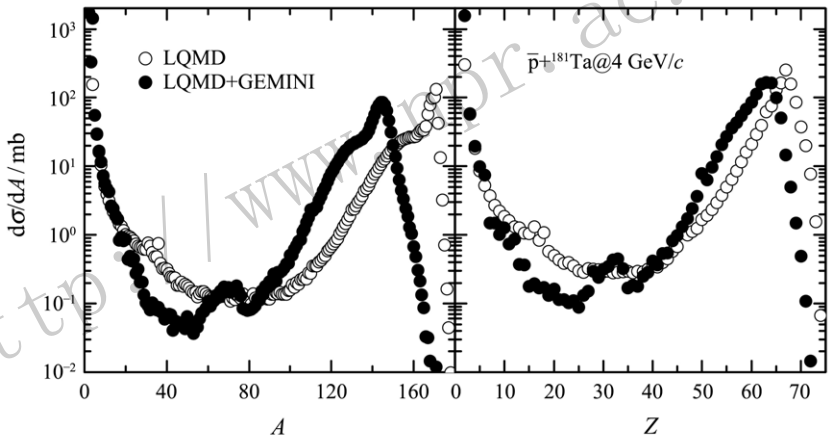

Fig. 3 Primary and final fragment distributions produced in the $\bar{p}$+^{181}Ta reaction at an incident momentum of 4 GeV/c.

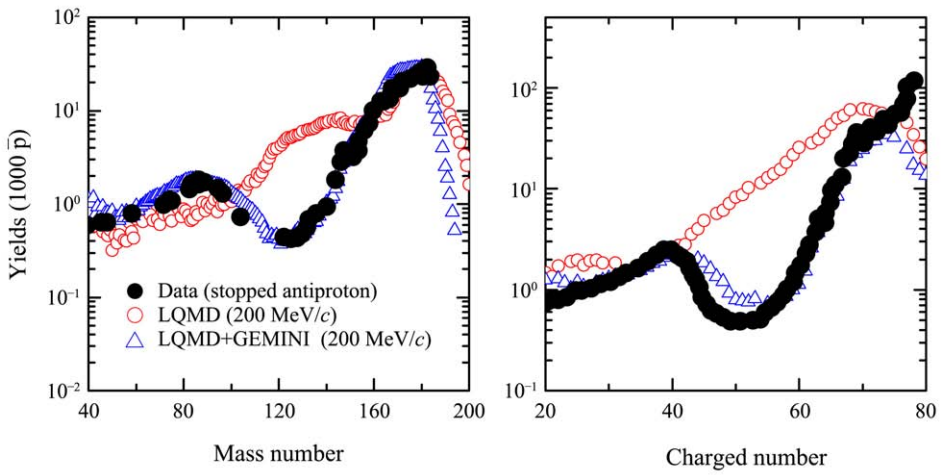

Fig. 4 (color online) Mass and charge distributions of fragments produced in the $\bar{p}$+^{197}Au reaction at an incident momentum of 200 MeV/c combined with the statistical decay code GEMINI. The mass yields from LEAR facility at CERN[17] are shown for comparison.

The phase-space structure of fragments in antiproton induced reactions would be helpful for the detector management in experiments. We assume a larger relative distance ($R_0 = 5$ fm) and the relative momentum similar to nucleonic ones ($P_0 = 200$ MeV/c) between hyperon and nucleon in constructing a hypernucleus, which is caused from the fact that the weakly bound of hypernucleus with a bigger rms (root-mean-square) radius. Shown in Fig. 5 is the kinetic energy distributions of nucleonic fragments and hot Λ-hyperfragments formed in collisions of $\bar{\mathrm{p}}$ on ^{20}Ne, ^{63}Cu and ^{181}Ta at an incident momentum of 4 GeV/c. The primary hyperfragments are formed within lower kinetic energies and the yields are roughly 3 order of magnitudes less than the case of the nucleonic fragments.

Properties of the hypernuclei would be significant

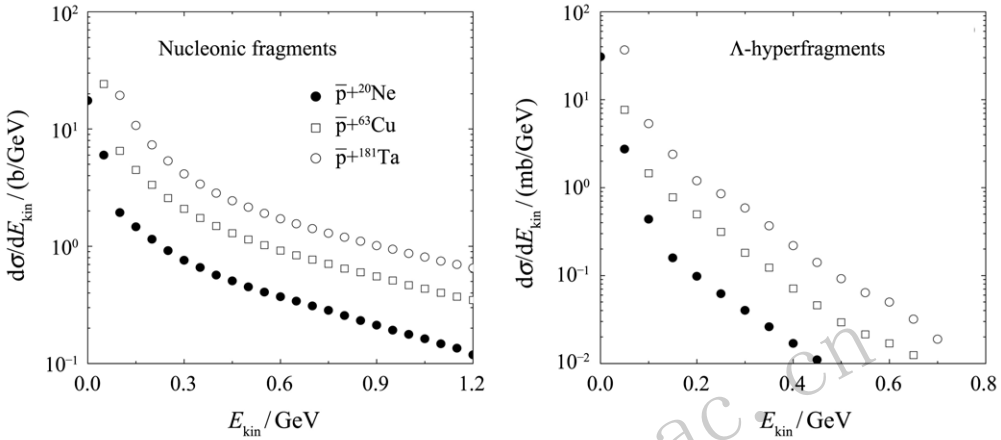

Fig. 5　(color online) Kinetic energy distributions of all fragments and primary Λ-hyperfragments formed in collisions of $\bar{\mathrm{p}}$ on ^{20}Ne, ^{63}Cu and ^{181}Ta at incident momentum of 4 GeV/c.

in understanding the Λ-Λ and $\bar{\Lambda}$-nucleon interactions, which are not well understood up to now. The antiproton-nucleus collisions would be a chance for producing the $s = -2$ and $s = 1$ hypernuclei. Shown in Fig. 6 is the mass and charged number distributions of hot hyperfragments with strangeness $s = -1$ ($_{\Lambda}$X), $s = 1$ ($_{\bar{\Lambda}}$X) and $s = -2$ ($_{\Lambda\Lambda}$X) in collisions of $\bar{\mathrm{p}}$+^{181}Ta at the incident momentum of 4 GeV/c. It is found that the Λ-hyperfragments spread the whole isotope range with the larger yields. The maximal cross sections for $s = -1$ and $s = -2$ hyperfragments are at the levels of 1 mb and 0.01 mb, respectively.

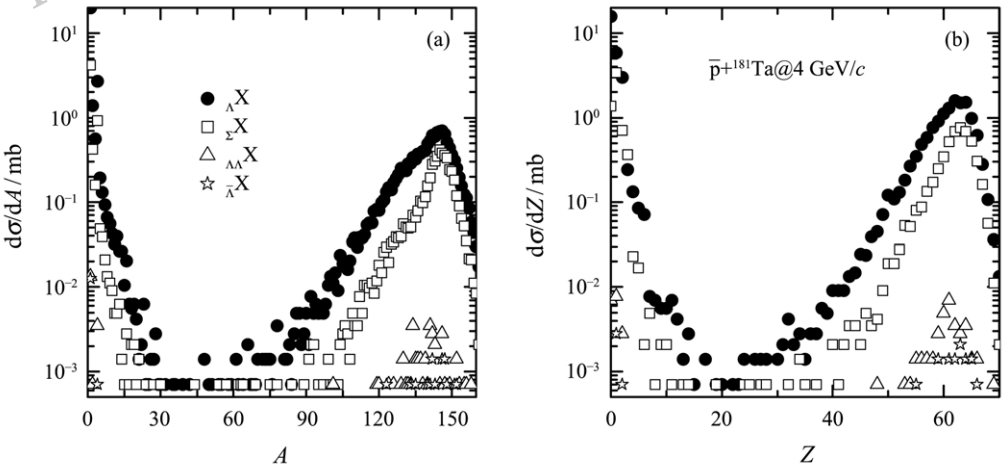

Fig. 6　Hyperfragments with strangeness $s = -1$ ($_{\Lambda}$X), $s = 1$ ($_{\bar{\Lambda}}$X) and $s = -2$ ($_{\Lambda\Lambda}$X) spectra as functions of atomic number (a) and charged number (b) in collisions of $\bar{\mathrm{p}}$ on ^{181}Ta at incident momentum of 4 GeV/c.

4　Conclusions

The formation mechanism of nucleonic fragments and hyperfragments in antiprotons induced reactions has been investigated within the LQMD transport model. The de-excitation of fragments is described with the help of the GEMINI approach. The available

data of the fragment production from the LEAR at CERN can be nicely reproduced with the combined approach. The energy released in the antiproton-nucleon annihilation is mainly deposited in the target nucleus via the pion-nucleon collisions. The production of hyperons is mainly attributed from the direct contribution of $N\overline{N}$ collisions, mesons induced and strangeness exchange reactions. Hyperfragments are formed within the narrower rapidities in comparison with nucleonic fragments and hyperons. Heavy hyperfragments close to the target-mass region have larger cross sections. The hypernuclei with strangeness $s=-2$ (double Λ-hypernucleus) and $s=1$ ($\overline{\Lambda}$-hypernucleus) would be feasible with the antiproton beams at PANDA (Antiproton Annihilation at Darmstadt, Germany) in the near future experiments.

References:

[1] RAFELSKI J. Phys Lett B, 1980, **91**: 281; RAFELSKI J, Phys Lett B, 1988, **207**: 371.

[2] GIBSON B E, HUNGERFORD E VIII. Phys Rep, 1995, **257**: 349.

[3] HASHIMOTO O, TAMURA H. Prog Part Nucl Phys, 2006, **57**: 564.

[4] DANYSZ M, PNIEWSKI J. Philos Mag, 1953, **44**: 348.

[5] CUGNON J, DENEYE P, VANDERMEULEN J. Nucl Phys A, 1989, **500**: 701; Phys Rev C, 1990, **41**: 1701.

[6] KO C M, YUAN R. Phys Lett B, 1987, **192**: 31.

[7] LARIONOV A B, PSHENICHNOV I A, MISHUSTIN I N, *et al.* Phys Rev C, 2009, **80**: 021601(R); Larionov A B. Nucl Sci Tech, 2015, **26**: S20506.

[8] BONDORF J P, BOTVINA A S, ILJINOV A S, *et al.* Phys Rep, 1995, **257**: 133.

[9] FENG Z Q, LENSKE H. Phys Rev C, 2014, **89**: 044617; FENG Z Q. Nucl Sci Tech, 2015, **26**: S20512; FENG Z Q. Phys Rev. C, 2016, **93**: 041601(R).

[10] FENG Z Q. Phys Rev C, 2011, **84**: 024610; FENG Z Q. Phys Rev C, 2012, **85**: 014604; FENG Z Q. Nucl Phys A, 2012, **878**: 3; FENG Z Q. Phys Lett B, 2012, **707**: 83.

[11] FENG Z Q. Phys Rev C, 2013, **87**: 064605; FENG Z Q. Nucl Phys A, 2013, **919**: 32; FENG Z Q, XIE W J, JIN G M, Phys Rev C, 2014, **90**: 064604.

[12] FENG Z Q, XIE W J, CHEN P H, *et al.* Phys Rev C, 2015, **92**: 044604.

[13] CÔNTÉ J, LACOMBE M, LOISEAU B, *et al.* Phys Rev Lett, 1982, **48**: 1319.

[14] BUSS O, GAITANOS T, GALLMEISTER K, *et al.* Phys Rep, 2012, **512**: 1.

[15] GOLUBEVA E S, ILJINOV A S, KRIPPA B V, *et al.* Nucl Phys A, 1992, **537**: 393.

[16] LARIONOV A B, GAITANOS T, MOSEL U. Phys Rev C, 2012, **85**: 024614.

[17] LUBINSKI P, GROCHULSKA A, VON EGIDY T, *et al.* Phys Rev C, 2002, **66**: 044616.

[18] CHARITY R J, MCMAHAN M A, WOZNIAK G J, *et al.* Nucl Phys A, 1988, **483**: 371.

反质子引起的核反应中碎裂机制和粒子产生

冯兆庆[1)]

(中国科学院近代物理研究所，兰州 730000)

摘要: 基于兰州量子分子动力学(LQMD)模型，系统研究了低能反质子引起的核反应中原子核碎裂机制和粒子产生。在LQMD输运模型中，考虑了反重子-重子、重子-重子和介子-重子碰撞可能产生的弹性散射、湮灭反应、电荷交换和非弹性散射。发展了并合模型，用于相空间构造初级碎片产生。处于激发态的碎片退激是基于统计模型描述。研究结果说明超子主要是由于奇异性交换产生；重碎片裂变会导致中等质量区域碎片产额增加；反质子引起的核反应有利于产生$s=-2$和$s=1$奇特超核，并给出了产生截面。

关键词: 兰州量子分子动力学模型；粒子产生；原子核碎裂；反质子引起的核反应

收稿日期: 2016-09-18

基金项目: 国家自然科学基金资助项目(11675226, 11175218)；国家重点基础研究发展计划项目(973计划)(2015CB856903)；中国科学院青年创新促进会专项基金

1) E-mail: fengzhq@impcas.ac.cn。